

How attractive and repulsive interactions affect structure ordering and dynamics of glass-forming liquids?

Ankit Singh and Yashwant Singh

Department of Physics, Banaras Hindu University, Varanasi-221 005, India.

(Dated: February 24, 2021)

The theory developed in our previous papers is applied in this paper to investigate the dependence of slowing down of dynamics of glass-forming liquids on the attractive and repulsive parts of intermolecular interactions. Through an extensive comparison of the behavior of a Lennard-Jones glass-forming liquid and that of its WCA reduction to a model with truncated pair potential without attractive tail, we demonstrate why the two systems exhibit very different dynamics despite having nearly identical pair correlation functions. In particular, we show that local structures characterized by number of mobile and immobile particles around a central particle markedly differ in the two systems at densities and temperatures where their dynamics show large difference and nearly identical where dynamics nearly overlap. We also show how the parameter $\psi(T)$ that measures the role of fluctuations embedded in the system on size of the cooperatively reorganizing cluster (CRC) and the crossover temperature T_a depend on the intermolecular interactions. These parameters stemming from the intermolecular interactions characterize the temperature and density dependence of structural relaxation time τ_α . The quantitative and qualitative agreements found with simulation results for the two systems suggest that our theory brings out the underlying features that determine dynamics of glass-forming liquids.

I. INTRODUCTION

In previous papers [1–3] of this series we introduced a new theory for slowing down of dynamics of fragile liquids on cooling. The theory identifies the local structural order that defines the cooperativity of relaxation and brings forth a temperature T_a and a temperature dependent parameter $\psi(T)$ that characterize temperature and density dependence of structural relaxation time. In Ref. [3], hereafter referred to as *I*, we reported results for the Kob-Anderson 80 : 20 binary Lennard-Jones (LJ) mixture [4] and compared them with simulation results [5, 6]. In this paper we investigate how different branches of intermolecular interaction potentials affect the local structural order and dynamics of supercooled liquids. In particular, we consider a model system in which particles interact via a purely repulsive pair potential formed by truncating the LJ potential at its minimum [7]; a potential known as the Weeks-Chandler-Anderson (WCA) binary mixture potential. The two potentials, the LJ and WCA, have same repulsive core but different attractive part; the LJ has an attractive tail while the WCA has no attraction. These models therefore offer an ideal benchmark for evaluating the role of repulsive and attractive interactions on the local structural order and on slowing down of dynamics of glass-forming liquids, and have been studied extensively over last several years [5, 6, 8–21]. We compare results of the two systems and identify causes that give rise a large difference in their local structural order and dynamics at lower liquid-like densities but almost identical results at sufficiently large densities.

It is almost universally accepted that the structure and thermodynamics of nonassociated liquids are primarily governed by the short range repulsive branch of pair potential while the attractive part of the potential provides, in the first approximation, a homogeneous cohesive back-

ground [7, 22, 23]. This led to formulation of theories in which properties of liquids are related to those of the repulsive core reference system, the attractive part of the potential being treated as a perturbation. The success of these perturbation theories [23] in predicting equilibrium properties of normal liquids led to expectation that the structure and dynamics of supercooled liquids should also be governed primarily by the local packing and the steric effects produced by the repulsive forces [24, 25]. This expectation was, however challenged by results found via molecular dynamics simulations by Berthier and Tarjus [5, 6] for the LJ and WCA mixtures. They found that while these systems exhibit nearly identical equilibrium structure, but at lower liquid-like densities and temperatures, very different dynamics: The value of structural relaxation time τ_α is much smaller in the WCA system than in the LJ ones at the same supercooled temperature indicating that the attractive forces have a nonperturbative effect on the relaxation dynamics. However, this large difference in values of τ_α decreases and ultimately vanishes as the density is significantly increased. Recent simulation studies [19, 20] done in the two and in three dimensions show similar effect of attractive interactions in slowing down of dynamics in the supercooled region.

The above findings bring forth the limitations [8, 9] of “microscopic” theories based on pair correlation function $g(r)$ [26–28]. For example, mode coupling theory was found to largely underestimate the difference in dynamics of the WCA and LJ systems [9]. This negative result led some authors to believe that $g(r)$ does not contain the physical information required to capture subtleties involved in dynamical slowdown and therefore any theory based on $g(r)$ is bound to fail [8]. It was suggested that the origin of this failure might be their neglect of higher order than pair correlations. Subsequent simulations of triplet correlation functions indicate that the

local ordering is more pronounced in the LJ system, an observation consistent with its slower dynamics [12]. This pronounced structure was, however, shown to arise due, to a good extent, to an amplification of the small discrepancies observed at the pair level [13]. Recently, Landes *et al.* [21] have used a standard machine learning algorithm to show that a properly weighted integral of $g(r)$ which amplifies the subtle differences between the two systems, correctly captures their dynamical differences. Local structure analysis using topological cluster classification [29] and Voronoi face analysis [12] also point to subtle structural difference. Using the configurational entropy as the thermodynamic maker via the Adam-Gibbs relation [30], Banerjee *et al.* [16–18] showed that the difference in dynamics of the WCA and LJ systems is due to difference in their configurational entropy. These results prompt one to ask whether a unified physical framework exists to understand the structure and dynamics and their relationship for systems such as the LJ and WCA glass forming liquids. Our goal here is to find answer to this question.

In Sec. II we give a brief account of our theory relevant to the present work. In Sec. III we calculate and report results for the WCA system and compare them with those found for the LJ system reported in I. Sec. IV is devoted to conclusion that emerged from similarity and contrast of results of the two systems and comparison with simulation findings.

II. THEORY:

Our theory provides a method to distinguish and calculate number of dynamically free, metastable and stable neighbors of a tagged (central) particle in a liquid at different temperatures and densities. This is achieved by including momentum distribution in the definition of $g(r)$ and using information of the configurational entropy S_c . The $g(r)$ of a binary mixture written in the center-of-mass coordinates is [1–3],

$$g_{\alpha\gamma}(r) = \left(\frac{\beta}{2\pi\mu}\right)^{\frac{3}{2}} \int d\mathbf{p} e^{-\beta(\frac{p^2}{2\mu} + w_{\alpha\gamma}(r))}. \quad (1)$$

Here $\beta = (k_B T)^{-1}$ is the inverse temperature measured in units of the Boltzmann constant k_B , \mathbf{p} is the relative momentum of a particle of mass $\mu = m/2$ (m being the mass of a particle of the liquid). The potential of mean force $w_{\alpha\gamma}(r) = -k_B T \ln g_{\alpha\gamma}(r)$ is a sum of the (bare) potential energy $u_{\alpha\gamma}$ and the system induced potential energy of interaction between a pair of particles of species α and γ separated by distance r [23]. The peaks and troughs of $g_{\alpha\gamma}(r)$ create, respectively, minima and maxima in $\beta w_{\alpha\gamma}(r)$ as shown in Fig. 1 of I. A region between two maxima, leveled as $i-1$ and i ($i \geq 1$) is denoted as i th shell and minimum of the shell as $\beta w_{\alpha\gamma}^{(id)}$. The value of i th maximum (barrier) is denoted as $\beta w_{\alpha\gamma}^{(iu)}$ and its location by r_{ih} .

All those particles in region of i th shell whose energies are less or equal to the barrier, $w_{\alpha\gamma}^{(iu)}$ would be trapped as they do not have enough energy to escape the barrier. These particles are considered as bonded (nonchemical) with the central particle. On the other hand, all those particles whose energies are higher than $\beta w_{\alpha\gamma}^{(iu)}$ are free to move around and collide with other particles. The number of bonded particles is found form a part of $g_{\alpha\gamma}(r)$ defined as [1, 3]

$$g_{\alpha\gamma}^{(ib)}(r) = 4\pi \left(\frac{\beta}{2\pi\mu}\right)^{3/2} e^{-\beta w_{\alpha\gamma}^{(i)}(r)} \int_0^{\sqrt{2\mu[w_{\alpha\gamma}^{(iu)} - w_{\alpha\gamma}^{(i)}(r)]}} \times e^{-\beta p^2/2\mu} p^2 dp, \quad (2)$$

where $w_{\alpha\gamma}^{(i)}(r)$ is the effective potential in the range of $r_{il} \leq r \leq r_{ih}$ of i th shell. Here r_{il} is value of r where $w_{\alpha\gamma}^{(i)}(r) = w_{\alpha\gamma}^{(iu)}$ on the left hand side of the shell (see Fig. 1 of I). The total number of particles that form bonds with the central particle of species α is

$$n_{\alpha}^{(b)} = 4\pi \sum_i \sum_{\gamma} \rho_{\gamma} \int_{r_{il}}^{r_{ih}} g_{\alpha\gamma}^{(ib)}(r) r^2 dr, \quad (3)$$

where summations are over all shells and over all species and ρ_{γ} is number density of γ component. The part of $g_{\alpha\gamma}(r)$ that corresponds to free particles is $g_{\alpha\gamma}^{(f)}(r) = g_{\alpha\gamma}(r) - g_{\alpha\gamma}^{(b)}(r)$.

Fluctuations embedded in the system (bath) activate some of these bonded particles, particularly those whose energies are close to the barrier height, to escape the shell. These particles are referred to as metastable (or m -) particles. The remaining bonded particles stay trapped in shells and form stable (long lived) bonds with the central particle. They are referred to as s -particles. This separation between the m - and s -particles is achieved via a parameter $\psi(T)$ which measures effect of the bath in activating bonded particles to escape the potential barrier. All those particles of i th shell whose energies lie between $\beta w_{\alpha\gamma}^{(iu)} - \psi$ and $\beta w_{\alpha\gamma}^{(iu)}$ escape the shell are m -particles. On the other hand, all those particles whose energies are lower than $[\beta w_{\alpha\gamma}^{(iu)} - \psi]$ remain trapped in the shell, are s -particles. The value of $\psi(T)$ in a normal (high temperature) liquid is one but decreases on cooling below a certain temperature denoted as T_a which depends on density ρ and on microscopic interactions between particles.

The number of s -particles at a given temperature and density is found from a part of $g_{\alpha\gamma}(r)$ defined as

$$g_{\alpha\gamma}^{(is)}(r) = 4\pi \left(\frac{\beta}{2\pi\mu}\right)^{3/2} e^{-\beta w_{\alpha\gamma}^{(i)}(r)} \int_0^{\sqrt{2\mu[w_{\alpha\gamma}^{(iu)} - \psi k_B T - w_{\alpha\gamma}^{(i)}(r)]}} \times e^{-\beta p^2/2\mu} p^2 dp, \quad (4)$$

where $w_{\alpha\gamma}^{(i)}(r)$ is in the range $r'_{il} \leq r \leq r'_{ih}$. Here r'_{il} and r'_{ih} are, respectively, value of r on the left and the right

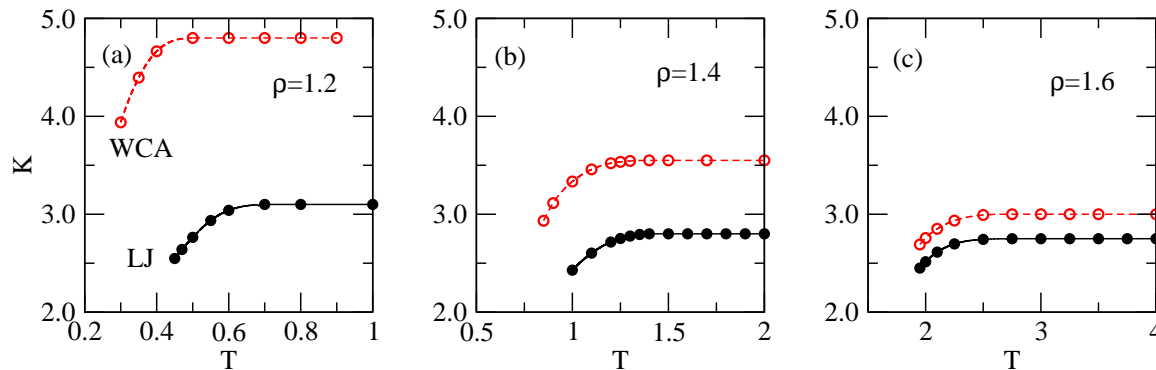


FIG. 1: Comparison of values of K for the LJ and WCA systems. These values were found when value of ψ was fixed to 1 at all temperatures. In both cases, K is constant above a density dependent temperature, T_a , and decreases from its constant value on cooling below T_a . Values of T_a of the two systems at different densities are given in Table I. Symbols represent calculated values and curves are least square fit.

hand side of the shell where $\beta w_{\alpha\gamma}^{(i)}(r) = \beta w_{\alpha\gamma}^{(iu)} - \psi$. The number of s -particles around a α particle is

$$n_{\alpha}^{(s)} = 4\pi \sum_i \sum_{\gamma} \rho_{\gamma} \int_{r_{ii}''}^{r_{ih}''} g_{\alpha\gamma}^{(is)}(r) r^2 dr. \quad (5)$$

The averaged number of s -particle bonded with a central particle in a binary mixture is

$$n^{(s)} = x_a n_a^{(s)} + x_b n_b^{(s)}, \quad (6)$$

where x_{α} is the concentration of species α .

The $n^{(s)}$, s -particles bonded with a central particle form a cooperatively reorganizing cluster (CRC). The number of particles in the cluster is related to the configurational entropy S_c through the Adam and Gibbs [30] relation,

$$n^{(s)}(T) + 1 = \frac{K}{S_c(T)}, \quad (7)$$

where K is a temperature independent constant. For an event of structural relaxation to take place the CRC has to reorganize irreversibly; The energy involved in this process is the effective activation energy $\beta E^{(s)}$ of relaxation. It is equal to the energy with which the central particle is bonded with $n^{(s)}$, s -particles and is given as

$$\beta E^{(s)}(T, \rho) = 4\pi \sum_i \sum_{\gamma} x_{\gamma} \rho_{\gamma} \int_{r_{ii}''}^{r_{ih}''} [\beta w_{\alpha\gamma}^{(iu)} - \psi(T) - \beta w_{\alpha\gamma}^{(i)}(r)] \times g_{\alpha\gamma}^{(is)}(r) r^2 dr, \quad (8)$$

where energy is measured from the effective barrier $\beta w_{\alpha\gamma}^{(iu)} - \psi(T)$. The structural relaxation time τ_{α} is obtained from the Arrhenius law,

$$\tau_{\alpha}(T, \rho) = \tau_0 \exp[\beta E^{(s)}(T, \rho)], \quad (9)$$

where τ_0 is a microscopic time scale.

The data of $g_{\alpha\gamma}(r)$ and S_c found from simulations and reported in Ref. [18] are used in the calculation.

III. RESULTS AND DISCUSSIONS

In this section we report results found for the WCA system and compare them with those reported in *I* for the LJ system at densities $\rho = 1.2, 1.4$ and 1.6 .

In Fig. 1 values of K calculated from Eqs. (4) – (7) with value of parameter $\psi(T)$ fixed at one at all temperatures T , are plotted as a function of T . In the figure we also plot values of K found in a similar way (see Fig. 2 of *I*) for the LJ system. We note that, in general, the temperature dependence of K of the WCA system is similar to the one found for the LJ system; K is constant above a temperature denoted as T_a and decreases from its constant value on cooling below T_a . As explained in *I*, the decrease in value of K below T_a is due to the unphysical condition that has been imposed on $\psi(T)$ by fixing its value equal to one for $T < T_a$. It is the temperature independent value of K , *i.e.* value of K found for $T > T_a$, that should be, as argued in *I*, used in Eq. (7). Values of K and T_a of both systems for three densities are listed in Table I. We note that value of K for the WCA system is higher at the same density than that for the LJ system. The difference, however, is found to decrease on increasing the density; while at $\rho = 1.2$ the difference is 1.70, it reduces to 0.25 at $\rho = 1.6$. This density dependent difference is a measure of the density dependent role of attractive interaction on configurations that is assessed

TABLE I: Value of constant K and the crossover temperature T_a of the LJ and WCA systems at different densities.

ρ	LJ		WCA	
	K	T_a	K	T_a
1.2	3.10	0.68	4.80	0.47
1.4	2.80	1.43	3.55	1.30
1.6	2.75	2.68	3.00	2.68

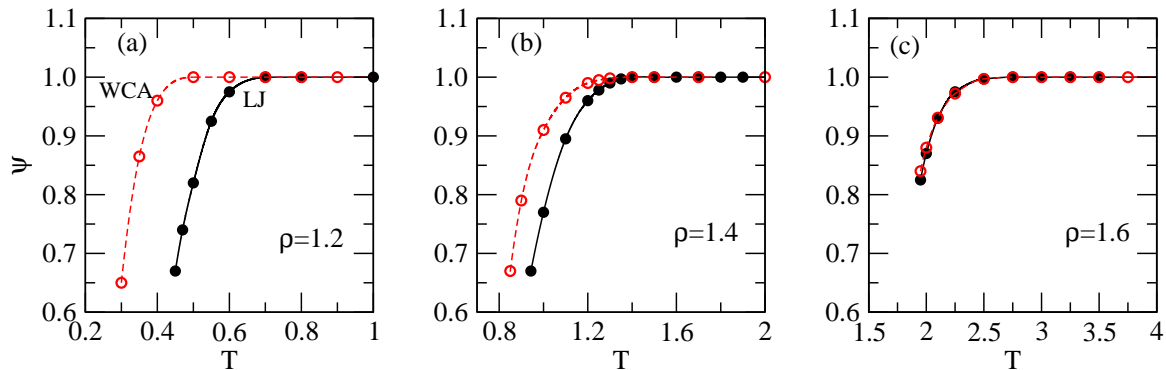


FIG. 2: Comparison of values of $\psi(T, \rho)$ of the two systems at different temperatures and densities. Symbols are calculated values and curves are least square fit. A large difference in values of $\psi(T, \rho)$ of the two systems for $\rho = 1.2$ below $T = 0.68$ is seen whereas for $\rho = 1.6$ values of $\psi(T)$ almost overlap at all temperatures.

by a CRC.

Values of K listed in Table I and of the configurational entropy S_c found from simulations [18] are used in Eq. (7) to calculate values of $n^{(s)}(T, \rho)$. From known values of $n^{(s)}(T, \rho)$ we determine $\psi(T, \rho)$ from Eqs. (4)–(6) for different values of T and ρ . We plot $\psi(T)$ vs T in Fig. 2. We note that for both systems, the high temperature value of $\psi(T)$ is equal to one and decreases rather sharply on cooling below T_a . The transition from the high temperature region to the low temperature region begins at T_a with a crossover region spreading over a narrow temperature width. Since the crossover region separates the high temperature region where slowing down of dynamics is slower from the low temperature region where slowing down of dynamics is faster, T_a can be taken as the crossover temperature. From Fig. 2 one finds that for $\rho = 1.2$ dynamics of the LJ system would start slowing down at faster rate for $T \leq 0.68$ whereas the slowing down of the WCA system would remain at slower rate till $T_a = 0.47$ on cooling. This results into a large difference in values of τ_α below $T = 0.68$ of the two systems. However, as ρ increases temperature dependence of dynamics of the two systems come closer as the difference in values of T_a decreases.

In Figs. (3–5) we compare radial distribution function $g_{\alpha\gamma}(r)$ and its different parts, $g_{\alpha\gamma}^{(f)}(r) = g_{\alpha\gamma}(r) - g_{\alpha\gamma}^{(b)}(r)$, $g_{\alpha\gamma}^{(m)}(r) = g_{\alpha\gamma}^{(b)}(r) - g_{\alpha\gamma}^{(s)}(r)$ and $g_{\alpha\gamma}^{(s)}(r)$, where $\alpha, \gamma = a, a$ and a, b (notations are of I) for the two systems at $(\rho, T) = (1.2, 0.5), (1.4, 1.0)$ and $(1.6, 2.0)$, respectively. As defined in Sec. II, $g_{\alpha\gamma}^{(f)}(r)$, $g_{\alpha\gamma}^{(m)}(r)$ and $g_{\alpha\gamma}^{(s)}(r)$ describe, respectively, distributions of free, m and s -particles around a central particle in a liquid. A look at these figures shows that while $g_{\alpha\gamma}(r)$ of the two systems in all cases nearly overlap, differences are seen in values of $g_{\alpha\gamma}^{(f)}(r)$, $g_{\alpha\gamma}^{(m)}(r)$ and $g_{\alpha\gamma}^{(s)}(r)$. In particular, first peaks of $g_{\alpha\gamma}^{(m)}(r)$ and $g_{\alpha\gamma}^{(s)}(r)$ in Fig. 3 show large difference at $\rho = 1.2$. The difference becomes less pronounced at $\rho = 1.4$ (Fig. 4) and almost disappears at $\rho = 1.6$ (Fig. 5). In all cases, the peak of $g_{\alpha\gamma}^{(m)}(r)$ is higher and $g_{\alpha\gamma}^{(s)}(r)$ is lower for the WCA system compared to those

for the LJ system. Since free and m particles are mobile whereas s particles are immobile, a particle in the WCA system is surrounded by a relatively larger population of mobile particles and a less population of immobile neighbors compared to those of the LJ system, leading to difference in their dynamical behavior. The subtle local structural order that defines the cooperativity of relaxation and remains hidden to experiments that measure pair correlation functions is defined in terms of $g_{\alpha\gamma}^{(s)}(r)$.

A useful information that shed light on the underlying features related to the local structural order and dynamics can be derived from the dynamical states of particles of the first shell surrounding the central particle as a function of temperature and density. In Fig. 6 we compare values of $n_1^{(f)}$, $n_1^{(m)}$ and $n_1^{(s)}$ as a function of $1/T$ for the two systems at different densities. Here the subscript 1 indicates the first coordination shell. In the figure solid lines indicate values for the LJ system and dashed lines for the WCA system. Letters f , m and s stand, respectively, for free, metastable and stable. We note that temperature dependence of number of particles of different dynamical states that surround the central particle in the two systems is, in general, similar. In both cases we find that at high temperatures most particles are free while a few are m -particles and a very few are s -particles. On cooling the systems, $n_1^{(m)}(T)$ remains nearly constant but $n_1^{(s)}(T)$ increases though slowly till $T = T_a$, but for $T < T_a$, $n_1^{(m)}(T)$ decreases and $n_1^{(s)}(T)$ increases with increasing rate at the cost of both free and m -particles. The rate is expected to increase rapidly on further lowering of temperatures, resulting into a rapid increase in number of s -particles and therefore in the cooperativity of relaxation. There is, however, a large difference particularly at low temperatures, in the number of particles of a given category of the two systems at $\rho = 1.2$; the difference decreases on increasing the density and almost disappears at $\rho = 1.6$.

One may prefer to use fraction of mobile (free plus m -particles) and immobile (localized) first neighbors de-

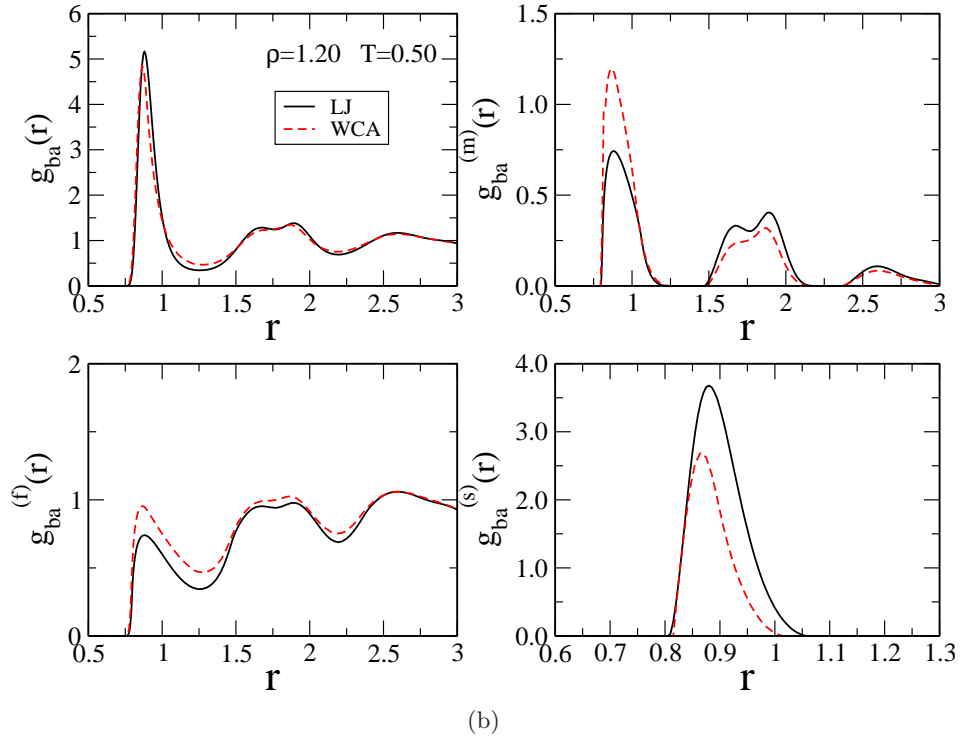
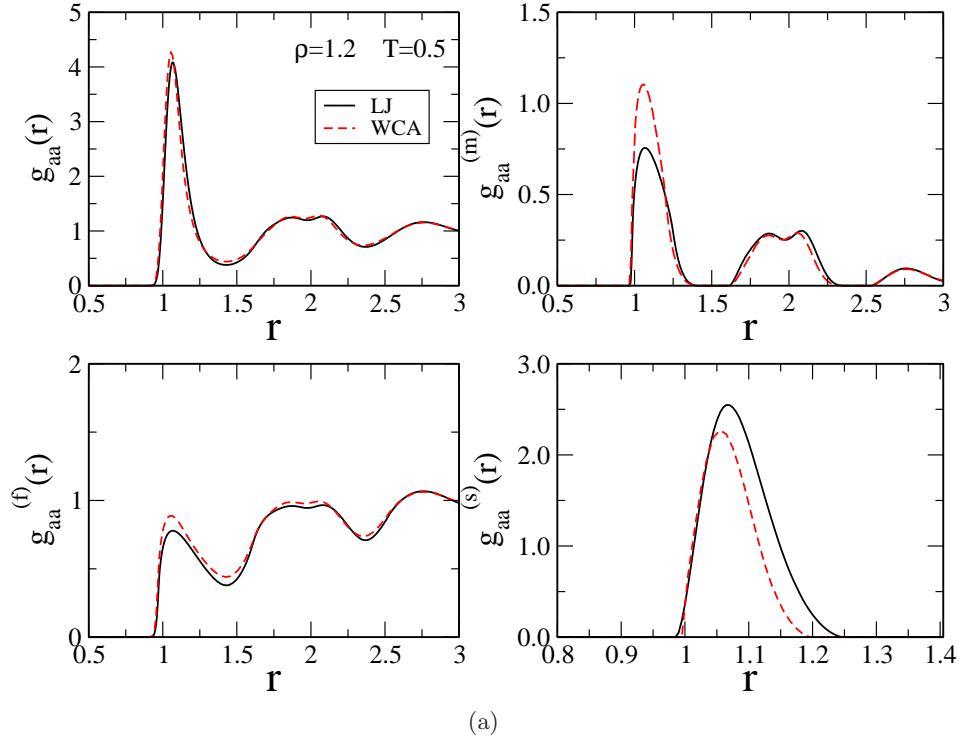


FIG. 3: Comparison of values of $g_{\alpha\gamma}(r)$ and its different parts $g_{\alpha\gamma}^{(f)}(r)$, $g_{\alpha\gamma}^{(m)}(r)$ and $g_{\alpha\gamma}^{(s)}(r)$ of the LJ (full lines) and WCA (dashed lines) for $\rho = 1.2$ and $T = 0.5$. In figure (a), $\alpha, \gamma = a, a$ and in (b), $\alpha, \gamma = a, b$. A large difference can be seen between values of $g_{\alpha\gamma}^{(s)}(r)$ and of $g_{\alpha\gamma}^{(m)}(r)$ of the two systems, while values of $g_{\alpha\gamma}(r)$ are nearly identical.

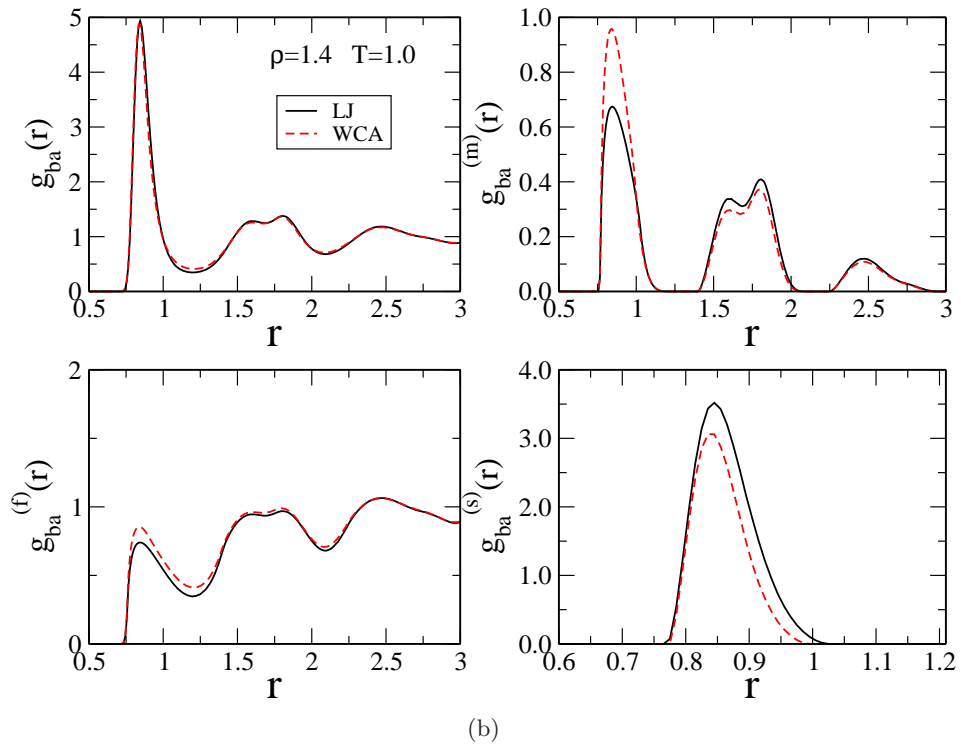
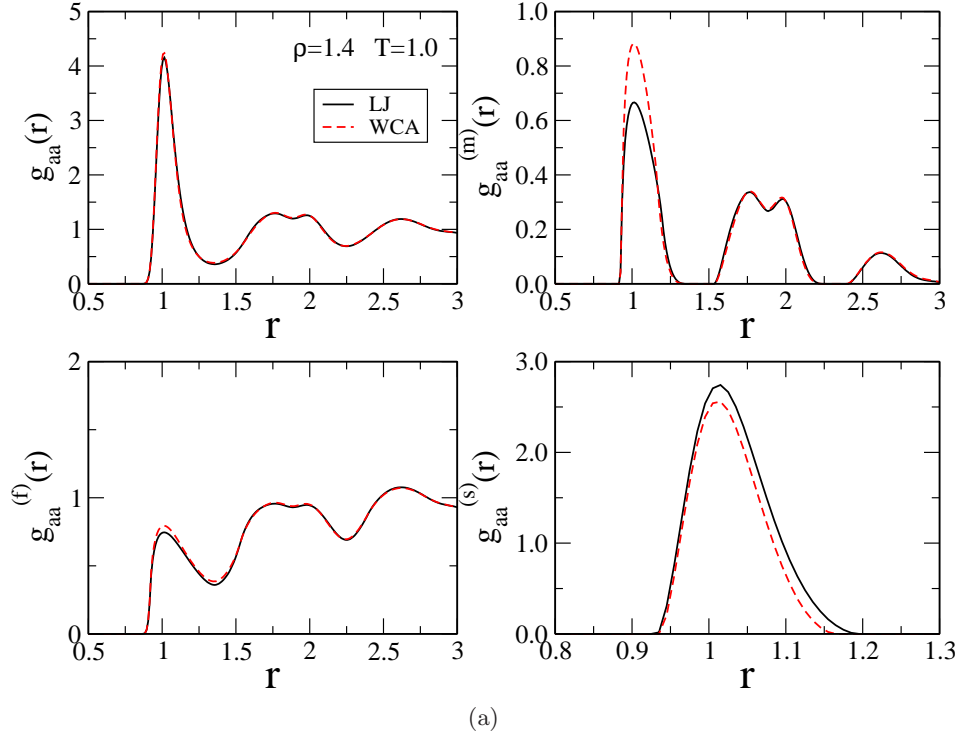


FIG. 4: Same as in Fig. 3 but for $\rho = 1.4$ and $T = 1.0$. A relatively small difference is seen between values of $g_{\alpha\gamma}^{(s)}(r)$ and of $g_{\alpha\gamma}^{(m)}(r)$ of the two systems compared to $\rho = 1.2$.

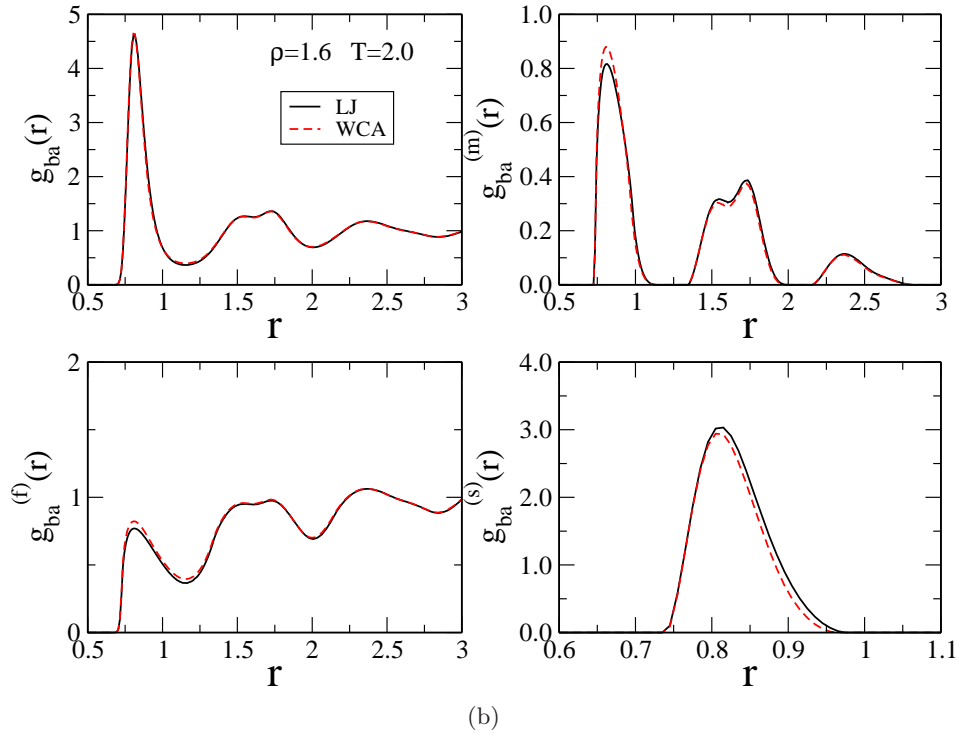
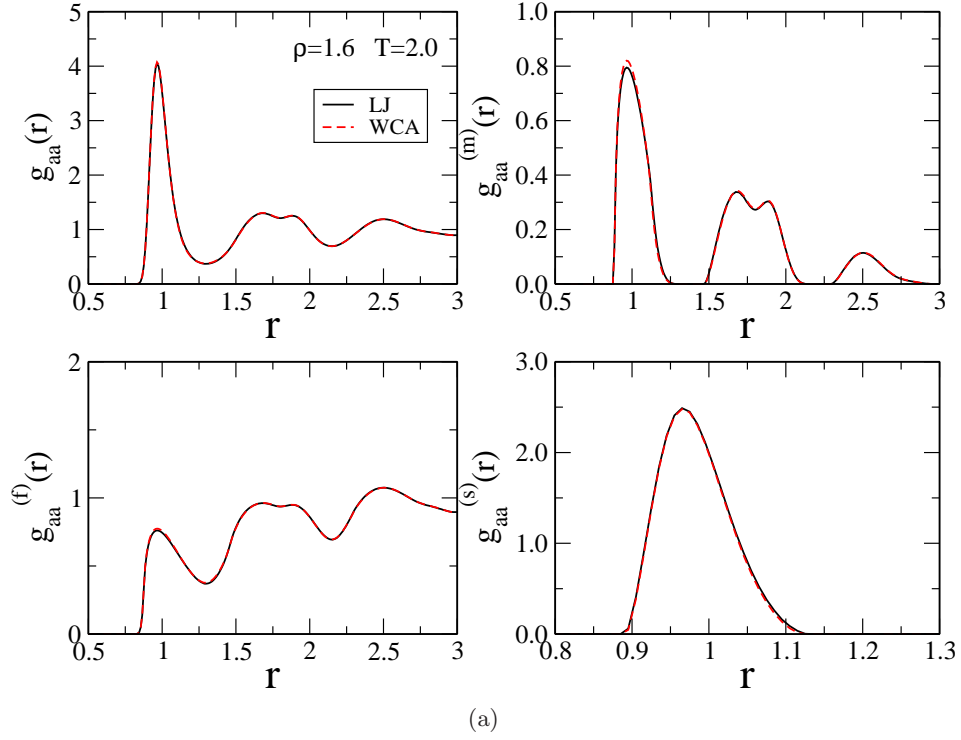


FIG. 5: Same as in Fig. 3 but for $\rho = 1.6$ and $T = 2.0$. Values of $g_{\alpha\gamma}(r)$ and of its components, $g_{\alpha\gamma}^{(f)}(r)$, $g_{\alpha\gamma}^{(m)}(r)$ and $g_{\alpha\gamma}^{(s)}(r)$ of the two systems are nearly identical.

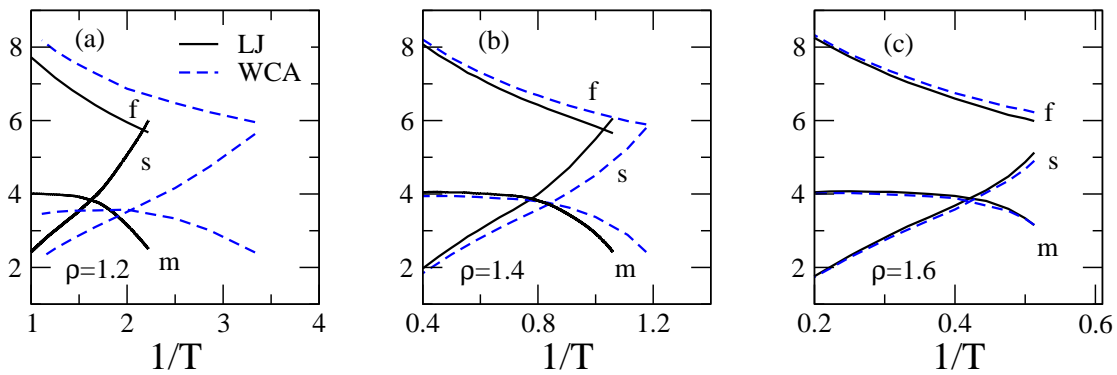


FIG. 6: Comparison of values of $n_1^{(f)}$, $n_1^{(m)}$ and $n_1^{(s)}$ as a function of $1/T$ for the two systems. Letters f , m and s stand, respectively, for free, metastable and stable and the subscript 1 stands for the first shell. Full lines represent values of the LJ system and dashed lines of the WCA system.

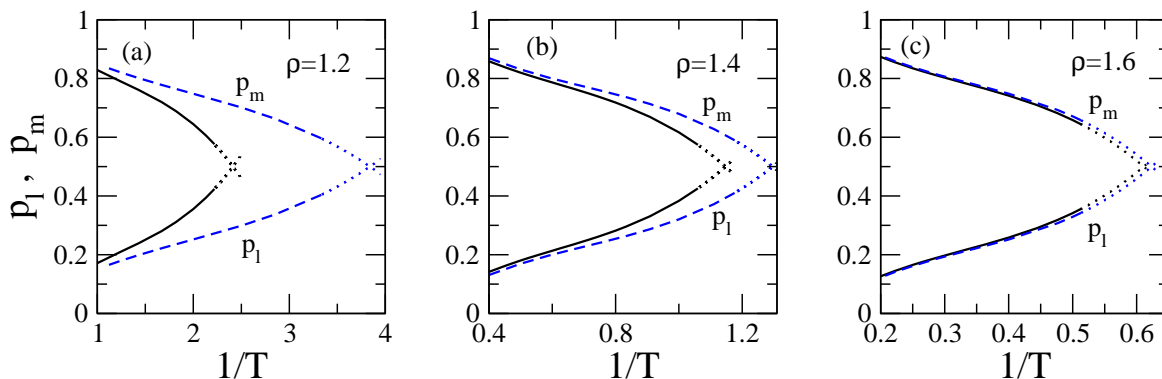


FIG. 7: Comparison of values of fraction of mobile, p_m , and immobile, p_l , (defined in the text) particles in the first shell around the central particle of the two systems. Line symbols are same as in Fig. 6. The dotted part of each line represents extrapolated values. The two curves of p_m and p_l meet at $T = T_{mc}$ where half of particles of the first neighbor become immobile.

defined, respectively, as $p_m(T) = \frac{n_1^{(f)}(T) + n_1^{(m)}(T)}{n_1^{(s)}(T)}$ and $p_l(T) = \frac{n_1^{(s)}(T)}{n_1^{(s)}(T)}$ to compare the local ordering relevant to dynamics. In Fig. 7 we plot and compare values of $p_m(T)$ and $p_l(T)$ of the two systems as a function of $1/T$. In the figure, lines (full for the LJ and dashed for the WCA) represent calculated values and dotted part of each line represents extrapolated values. A glance at this figure reveals how the local ordering defined in terms of the fraction of mobile and immobile particles around the central particle in the two systems compare with each other at different densities. The extrapolated parts of lines representing $p_m(T)$ and $p_l(T)$ meet at a temperature (denoted as T_{mc}) where half of the neighbors become immobile. The values of T_{mc} found for densities $\rho = 1.2$, 1.4 and 1.6 for the LJ system are, respectively, 0.41, 0.87 and 1.64 whereas the corresponding values for the WCA system are 0.26, 0.77 and 1.62. The large difference in

the temperature dependence of $p_m(T)$ and $p_l(T)$ and values of T_{mc} found at $\rho = 1.2$ that decreases on increasing the density further explains why dynamics of the two systems show large difference at $\rho = 1.2$ but become almost identical at $\rho = 1.6$.

The effective activation energy $\beta E^{(s)}(T, \rho)$ and the relaxation time $\tau_\alpha(T, \rho)$ calculated, respectively, from Eqs. (8) and (9) are plotted in Fig. 8. In Fig. 8(a) values of $\beta E^{(s)}$ of the two systems are compared as a function of $1/T$. In Fig. 8(b) we compare values of τ_α/τ_0 of the two systems with each other and with values found from simulations [5, 6]. An excellent agreement is found with simulation values for all densities for both systems.

The density dependence of T_a is shown in Fig. 9. In the figure, circles - full for the LJ and open for the WCA - denote calculated values and the curves - full line for the LJ and dashed line for the WCA - represent fit with a power law form $T_a = a_0 \rho^\gamma$. In case of the LJ system, $a_0 = 0.287$ and $\gamma = 4.757$ while in case of the WCA,

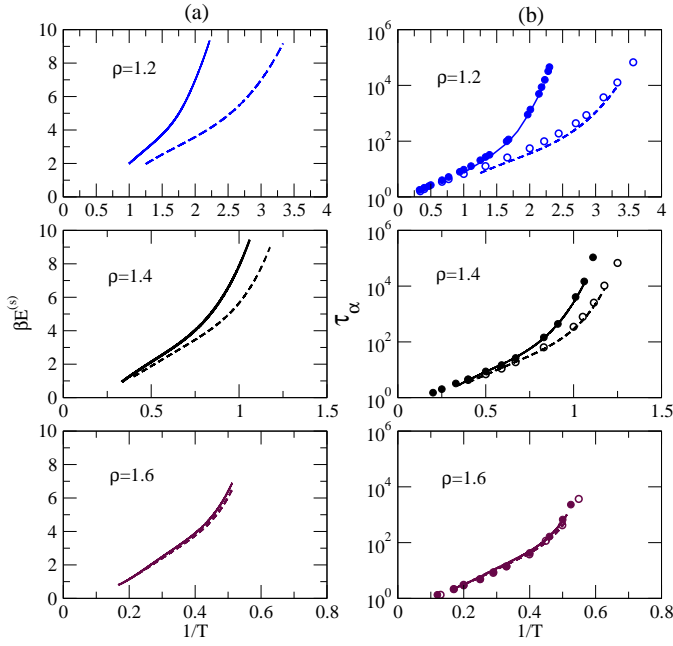


FIG. 8: Comparison of values of activation energy $\beta E^{(s)}$ for the relaxation in column (a) and the relaxation time in column (b) as a function of $1/T$ at three densities of the two systems. Curves (full for the LJ and dashed for the WCA) represent calculated values and circles (full for the LJ and open for the WCA) in column (b) represent simulation values.

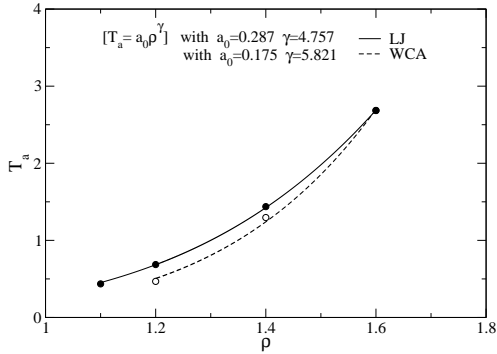


FIG. 9: Comparison of density dependence of the temperature T_a of the two systems. Circles (full for the LJ and open for the WCA systems) represent calculated values (given in Table I) and curves (full for the LJ and dashed for the WCA) represent fit $T_a = a_0 \rho^\gamma$ with $\gamma = 4.757$ and 5.821 , respectively for the LJ and WCA systems.

$a_0 = 0.175$ and $\gamma = 5.821$. It was shown in *I* that when $\psi(T)$, τ_α , $\beta E^{(s)}$, etc., are plotted as a function of T_a/T (or T/T_a) the data collapse on master curves. However, in case of the WCA such a collapse fails in agreement with result found from simulations [5, 6]. We plot calculated values (shown by lines) and simulation values by symbols

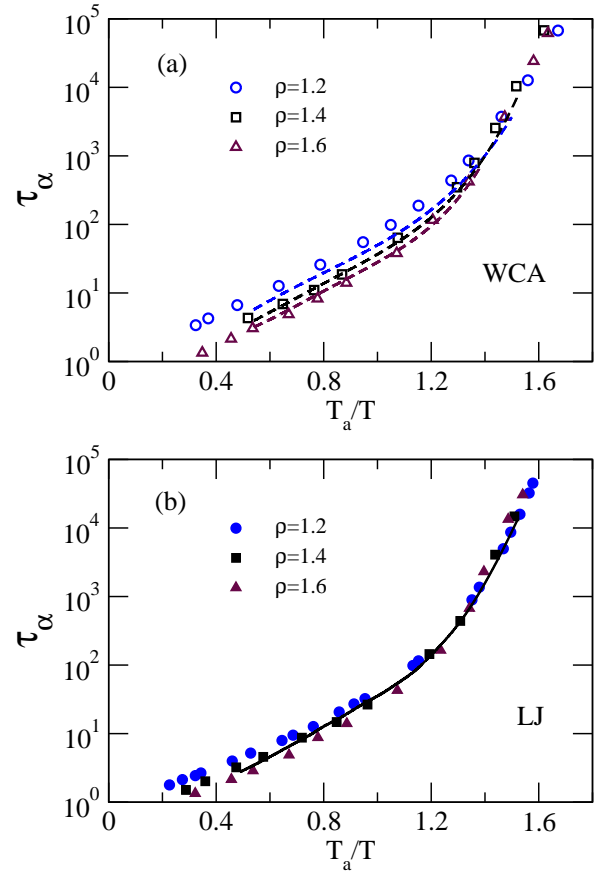


FIG. 10: Comparison of collapse of calculated (lines) and simulation (symbols) data of τ_α of the two systems as a function of T_a/T . While in the case of LJ system (b) good collapse takes place, in case of the WCA (a), both the calculated as well as simulation values fail to collapse on one curve.

of τ_α/τ_0 as a function of T_a/T for densities $\rho = 1.2, 1.4$ and 1.6 in Fig. 10(a) for the WCA system and in 10(b) for the LJ system. While in case of the LJ system a good collapse of data happens, in case of the WCA both the calculated as well as simulation values fail to collapse on one curve and therefore violates the density scaling relation; a feature attributed to the fact that the WCA liquid follows an “isomorph” different from that of the LJ liquid [10, 11].

IV. CONCLUSION

Through an extensive comparison of the behavior of a LJ glass forming liquid and its WCA reduction to a model with truncated potential without attractive tail, we have shown that our theory brings out several underlying features that characterize slowing down of dynamics of these systems. It is shown that though the equilibrium static structures measured by the pair correlation functions, $g_{\alpha\gamma}(r)$ of the two systems are nearly identical,

there is a marked difference, particularly at low densities and low temperatures, in their components representing free, metastable and stable particles distributed in coordination shells around a central particle. In particular, the parameters $p_m(T)$ and $p_l(T)$ which define, respectively, the fraction of mobile and immobile first neighbors and plotted in Fig. 7 provide information about the local structure relevant to dynamics.

The other intrinsic parameters stemming from the intermolecular interactions and which explain why slowing down of dynamics of the two systems are qualitatively and quantitatively different at lower densities and lower temperatures but nearly identical at higher densities and higher temperatures are $\psi(T)$ and the crossover temperature T_a . The value of parameter $\psi(T)$ which measures the effect of fluctuations embedded in the system on stabilizing the shape and size of CRC, takes a turn from its high temperatures value of 1 at $T = T_a$ and starts decreasing rather sharply as T is lowered. There is a one-to-one correspondence between the crossover region of $\psi(T)$ and τ_α (for more details see *I*) indicating the significance of embedded fluctuations on temperature and density dependence of local structure and dynamics. The temperature T_a separates the high temperature behavior region where slowing down of dynamics is slower from a

low temperatures region where slowing down of dynamics is faster. Both ψ and T_a depend on details of intermolecular interactions. Whenever the attractive part of intermolecular interaction is effective in suppressing entropy driven escapes of particles out of shells, the crossover temperature T_a shifts to higher temperatures resulting into slowing down of dynamics at faster rate than in absence of the attractive part. The reason why value of τ_α for $\rho = 1.2$ is much smaller in the WCA system, say at $T = 0.5$, than the LJ ones, lies in the difference in their values of T_a (see Table I). The quantitative and qualitative agreements found with simulation results for the two systems suggest that our theory accurately describes the intricate nature of the connection between the local structural order and dynamics arising due to attractive and repulsive interactions in glass-forming liquids.

ACKNOWLEDGMENTS

We thank Dr. S. M. Bhattacharyya for helpful discussions and for providing simulation data of pair correlation functions $g_{\alpha\gamma}(r)$ and configurational entropy S_c . One of us (A.S.) acknowledges research fellowship from the Council of Scientific and Industrial Research, New Delhi, India.

-
- [1] A. Singh and Y. Singh, Phys. Rev. E **99**, 030101(R) (2019).
- [2] A. Singh and Y. Singh, arXiv:1909.02734.
- [3] A. Singh, S. M. Bhattacharyya, and Y. Singh, arXiv:2011.09185.
- [4] W. Kob and H. C. Andersen, Phys. Rev. Lett. **73**, 1376 (1994).
- [5] L. Berthier and G. Tarjus, Phys. Rev. Lett. **103**, 170601 (2009).
- [6] L. Berthier and G. Tarjus, J. Chem. Phys. **134**, 214503 (2011).
- [7] J. D. Weeks, D. Chandler, and H. C. Andersen, J. Chem. Phys. **54**, 5237 (1971).
- [8] L. Berthier and G. Tarjus, Eur. Phys. J. E **34**, 96 (2011).
- [9] L. Berthier and G. Tarjus, Phys. Rev. E **82**, 031502 (2010).
- [10] J. C. Dyre, J. Phys. Chem. B **118**, 10007 (2014).
- [11] U. R. Pedersen, T. B. Schröder, and J. C. Dyre, Phys. Rev. Lett. **105**, 157801 (2010).
- [12] D. Coslovich, Phys. Rev. E **83**, 051505 (2011).
- [13] D. Coslovich, J. Chem. Phys. **138**, 12A539 (2013).
- [14] G. M. Hocky, T. E. Markland, and D. R. Reichman, Phys. Rev. Lett. **108**, 225506 (2012).
- [15] Z. E. Dell and K. S. Schweizer, Phys. Rev. Lett. **115**, 205702 (2015).
- [16] A. Banerjee, S. Sengupta, S. Sastry, and S. M. Bhattacharyya, Phys. Rev. Lett. **113**, 225701 (2014).
- [17] M. K. Nandi, A. Banerjee, C. Dasgupta, and S. M. Bhattacharyya, Phys. Rev. Lett. **119**, 265502 (2017).
- [18] A. Banerjee, M. K. Nandi, S. Sastry, and S. M. Bhattacharyya, J. Chem. Phys. **145**, 034502 (2016).
- [19] J. Chattoraj and M. P. Ciamarra, Phys. Rev. Lett. **124**, 028001 (2020).
- [20] H. Tong and H. Tanaka, Phys. Rev. Lett. **124**, 225501 (2020).
- [21] F. P. Landes, G. Biroli, O. Dauchot, A. J. Liu, and D. R. Reichman, Phys. Rev. E **101**, 010602 (2020).
- [22] D. Chandler, J. D. Weeks, and H. C. Andersen, Science **220**, 787 (1983).
- [23] J. P. Hansen and I. R. McDonald, *Theory of Simple Liquids*, 3rd ed. (Academic, Burlington, 2006).
- [24] S. D. Bembenek and G. Szamel, J. Phys. Chem. B **104**, 10647 (2000).
- [25] T. Young and H. C. Andersen, J. Phys. Chem. B **109**, 2985 (2005).
- [26] W. Götze, *Complex Dynamics of Glass-Forming Liquids: A Mode-Coupling Theory* (Oxford University Press, Oxford, 2008).
- [27] T. R. Kirkpatrick and P. G. Wolynes, Phys. Rev. A **35**, 3072 (1987).
- [28] K. S. Schweizer, J. Chem. Phys. **123**, 244501 (2005).
- [29] J. Taffs, A. Malins, S. R. Williams, and C. P. Royall, J. Chem. Phys. **133**, 244901 (2010).
- [30] G. Adam and J. H. Gibbs, J. Chem. Phys. **43**, 139 (1965).